



Iron–Copper Bimetallic Nanoparticle for the Removal of Disinfection By-products: Optimization, Kinetic Study, and Life Cycle Assessment

Kubra Ulucan-Altuntas · Ahmed El Hadki ·
Levent Bilgili · Afşın Y. Çetinkaya ·
S. Levent Kuzu · Eyup Debik

Received: 7 March 2022 / Accepted: 17 June 2022 / Published online: 7 July 2022
© The Author(s) 2022

Abstract Since the early twentieth century, disinfecting water has been an essential process to prevent the introduction of harmful organisms, especially pathogenic organisms. Due to the reaction between anthropogenic contaminants present in water and the chemicals used to disinfect water, compounds known as disinfection by-products (DBPs) are formed during the water disinfection process. Chlorination, the most dominant water disinfection method, produces DBPs that have drawn a lot of attention and health concerns. The most commonly used removal technology for trichloromethane (TCM) is adsorption, and the use of activated

carbon, iron oxides, and nanoparticles has been widely investigated. Studies have found that using nano-zero valent iron with nano-catalytic metals (Cu, Ni etc.) to synthesize bimetallic nanoparticles increases the removal of organic pollutants. The current study investigates the adsorption of trichloromethane (TCM) by synthesized Fe/Cu bimetallic nanoparticles. The response surface methodology (RSM) was used to investigate the effect of independent variables on the removal of TCM. According to the CCD results, TCM concentration and reaction time were determined as the most effective parameters. The lowest TCM concentrations have low removal efficiencies, while the lowest TCM concentration (50 µg/L) can be removed up to 60%. The highest TCM concentration can be 500 µg/L to achieve a removal below the limits with 500 mg/L Fe/Cu concentration and 24 min of reaction time. Life cycle assessment (LCA) was applied to Fe/Cu nanoparticle synthesis, and results indicated that the highest environmental impact was from the mixture of reactant stage.

K. Ulucan-Altuntas
Department of Chemical Sciences, University of Padua,
Padua, Italy

K. Ulucan-Altuntas (✉) · A. E. Hadki · A. Y. Çetinkaya ·
S. L. Kuzu · E. Debik
Department of Environmental Engineering, Yildiz
Technical University, Istanbul, Turkey
e-mail: kubra.altuntas@unipd.it

A. E. Hadki (✉)
Laboratory of Spectroscopy, Molecular Modeling,
Materials, Nanomaterials, Water, and Environment,
Department of Chemistry, Faculty of Sciences,
Mohammed V University, LS3MN2E-CERNE2D Rabat,
Morocco
e-mail: el.hadki.ahmed@gmail.com

L. Bilgili
Department of Naval Architecture and Marine
Engineering, Bandirma Onyedü Eylül University, Balıkesir,
Turkey

Keywords Chloroform · Nanoparticles · Nano-zero valent iron · Response surface methodology · Life cycle assessment

1 Introduction

Disinfection of drinking water and wastewater with chlorine is a common practice worldwide. The problem is that chlorine can react with the natural organic

matter (NOM) present during the disinfection process to form damaging disinfection by-products (DBPs) (Benítez et al., 2021; Domínguez Henao et al., 2018; Ulucan-Altuntas et al., 2020), chloroform (CHCl_3), bromodichloromethane (CHCl_2Br), dibromochloromethane (CHClBr_2), and bromoform (CHBr_3) (G. da C. Cunha, L.P.C. Romão, M.C. Santos, B.R. Araújo, S. Navickiene & V.L. de Pádua, 2010). It has been reported in various studies that these by-products formed after chlorination have dangerous and carcinogenic effects (Sriboonnak et al., 2021; Zhang et al., 2012). Therefore, practical, cost-effective, and straightforward technology is required to remove these substances from water.

The commonly used, simplest, and least expensive technology for removing micropollutants like DBPs is adsorption technology (G. da C. Cunha, L.P.C. Romão, M.C. Santos, B.R. Araújo, S. Navickiene & V.L. de Pádua, 2010; Lu et al., 2006; Matsui et al., 2015). However, adsorption by activated carbon is limited in the effective removal of brominated compounds and trihalomethanes (THMs). Hence, with the rapid advancement of nanotechnology, iron nanoparticles have recently attracted much attention and have emerged as a new class of adsorbent by having advantages of high surface area to volume ratio, being environmentally friendly, and being cost-effective (Tural et al., 2021; Ulucan-Altuntas & Debik, 2018). Nanoscale ZVI became the most promising material in in situ remediation towards a wide range of organic and inorganic contaminants with significant removal efficiency (Dong et al., 2016; Kahraman et al., 2022). Despite this, practical limitations have been discovered, including poor stability and agglomeration tendency due to magnetic forces and oxide layers forming on the surface of nano-zero valent iron (nZVI) that can lead to low reaction activity (Ulucan-Altuntas, 2019).

Synthesis of iron-based bimetallics by loading another transition metal on the surface of nZVI to effectively increase the reactivity of nZVI is among the topics investigated. The addition of transition elements can accelerate the corrosion of nZVI and improve the reaction performance. In this sense, among the developed approaches to overcome the inconveniences and limitations associated with nZVI is loading the nZVI surface with another metal (e.g., Ni, Pd, Cu) to form bimetallic nanoparticles (BNPs) (Venkateshaiah et al., 2021). In this study, copper was chosen because it is cheaper and widely available

compared to other metals. It is suggested by many researchers that the synergistic effect of iron and copper increases removal. Dong et al. (2022) studied sulfamethazine degradation by Fe/Cu nanoparticles activated by sulfite and reported that Fe/Cu nanoparticles were superior than nZVI in sulfamethazine degradation with sulfite (Dong et al., 2022). Fe/Cu nanoparticles were also used for phenol degradation via Fenton-like process (Xia et al., 2022).

Life cycle assessment (LCA) can successfully determine the environmental impacts of disinfection systems. Environmental impacts of different categories are assessed through LCA, a standardized methodology (Bilgili et al., 2019). In addition, LCA provides quantitative information to enable decision-making during strategic planning of water reuse in water treatment and disinfection processes (Çetinkaya, 2020).

The overarching objective of this research is to examine the adsorption efficiency of Fe/Cu bimetallic nanoparticles for TCMs. The response surface methodology was applied to determine the optimum adsorption conditions and interactive influences of effective parameters (Fe/Cu dosage, initial concentration, pH, and contact time). Finally, LCA calculations were executed to determine the holistic effects of the experimental setup.

2 Material and Methods

2.1 Experimental Study

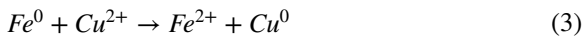
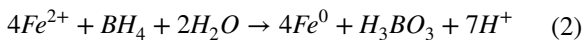
TCM adsorption studies by bimetallic Fe/Cu nanoparticles were investigated in 100 mL sample volume and at a fixed temperature of 20 °C. All the experiments were performed in a shaker (GLF model 82,362, Turkey), and in order to work at a fixed temperature, the shaker was placed in an incubator (WTW model TS1006-I, Turkey). The samples were shaken at 100 rpm to obtain a homogenous mixing of Fe/Cu nanoparticles in aqueous solutions. The adsorbent suspension was centrifuged after a determined time by the Hettich brand Rotofix 32 A Zentrifugen centrifuge. The initial and effluent samples were analyzed in gas chromatography equipped with an ECD detector and a head-space according to standard method SM 6232 D. The removal efficiency of TCM by bimetallic Fe/Cu nanoparticles was estimated using Eq. (1):

$$R\% = \frac{C_0 - C_e}{C_0} \times 100 \tag{1}$$

where R (%) is the TCM removal efficiency (%), C_0 is the initial concentration of TCM (mg/L), and C_e is the final concentration of TCM (mg/L).

2.2 Fe/Cu Bimetallic Nanoparticle Synthesis

Copper-containing iron bimetallic nanoparticles (Fe/Cu) were synthesized based on the modified nZVI synthesis method (Ulucan-Altuntas and Debik 2018; Ulucan-Altuntas and Kuzu, 2019). The ratio of copper was optimized in the previous study as 5% (Cu:Fe) (Ulucan-Altuntas and Kuzu, 2019). According to this method, the calculated amount of copper nitrate was added to FeSO₄ solution before synthesizing according to Eq. (2) and Eq. (3):



The calculated amount of BH₄ was added dropwise to the prepared solution with 25 ml/min flow-rate. The synthesized Fe/Cu bimetallic nanoparticle was examined for particle size with Malvern Zetasizer and found 82 nm.

2.3 Characterization of Nanoparticle

The X-ray diffraction patterns of the synthesized Fe/Cu nanoparticles were studied under CuKα radiation operated at 45 kV and 40 mA (λ = 1.54060 Å) and scanned for 15–90° (PANalytical X’pert Pro). The scanning electron microscopy (SEM) imaging was conducted using Tecnai G2 F20 S-TWIN.

2.4 Response Surface Methodology

In an experimental design, it is possible to describe how factors (input variables) interact with the change of the response variable (dependent variable) as a result of these factors. It is a unique method in defining process variables by reducing process variables and ensuring process optimization. According to the response surface methodology, there is three commonly used experimental design methods, and central composite design (CCD) is the most commonly used design. This model can be expressed with the following equation (Eq. 4):

$$Y = \beta_0 + \sum_{i=1}^k \beta_i X_i + \sum_{i=1}^k \beta_{ii} X_i^2 + \sum_{i < j} \beta_{ij} X_i X_j + e(X_1, X_2, \dots, X_k) \tag{4}$$

where Y is the dependent response, X_i is independent variables, β_0 is an intersection, and $\beta_i, \beta_{ii}, \beta_{ij}$ are the linear, multiplies, and squares of the independent variables’ coefficients, respectively.

The maximum acceptable concentration for TCM was limited by 60 µg/L by the World Health Organization (WHO) (Xu et al., 2017). Therefore, in the current study, the concentration of TCM was selected higher than this limit concentration, and 3-factor 5-level CCD was prepared as given in Table 1. TCM concentration (x_1 , 50–550 µg/L), Fe/Cu concentration (x_2 , 50–650 mg/L), and reaction time (x_3 , 10–90 min) were selected as independent variables. The coding of the variables was done according to α and selected as ± 2 via Eq. 5:

$$\alpha = \frac{x_i - x_{cp}}{\Delta x_i} \tag{5}$$

where is α the coded value, x_i and x_{cp} are the original value and its center point, respectively, and Δx_i is the value of the variable change step. One can define the α

Table 1 Working matrix of CCD for TCM adsorption

Independent variables	Factors		Levels in RSM			
	X_j	$\alpha = -2$	-1	0	1	$\alpha = +2$
TCM Concentration (µg/L)	x_1	50	175	300	425	550
Fe/Cu Concentration (mg/L)	x_2	50	200	350	500	650
Reaction time (min)	x_3	10	30	50	70	90

value as the distance between each axial point and the center in CCD. The coded and uncoded values of independent variables can be found in Table 1. The experiments were designed in CCD as given in Table 4.

2.5 Life Cycle Assessment

LCA is an innovative approach used in the holistic assessment of the environmental, economic, and social impacts of all product system processes, which is a definition for all types of products or services used in LCA calculations. The comprehensive methodology LCA process is given in ISO 14044 (Finkbeiner et al., 2006). LCA calculations can determine which process of a product system is more effective than others in environmental terms, and necessary improvements can be directed to the proper process. LCA consists of four sub-processes, which are related to each other during all assessments: (1) goal and scope definition, in which the system boundaries and functional unit are determined; (2) inventory analysis, in which the materials and energy consumed are determined precisely; (3) impact assessment, in which the impacts of the product system are calculated by the help of the appropriate method; and (4) interpretation, which covers all other sub-processes and is used for the final assessment (Hauschild et al., 2017).

SimaPro 9.3.0.2 software and ReCiPe 2016 are used for the LCA calculations in this study. In this method, global warming; stratospheric ozone depletion; ionizing radiation; ozone formation; fine particulate matter formation; terrestrial acidification; freshwater and marine eutrophication; terrestrial, freshwater, and marine ecotoxicity; human carcinogenic toxicity; human non-carcinogenic toxicity; land use, mineral, and fossil resource scarcity; and water consumption midpoint categories can be calculated (Cetinkaya et al., 2022; Çetinkaya et al., 2018).

3 Results and Discussion

3.1 Characterization of Synthesized Fe/Cu Nanoparticle

Fe/Cu nanoparticles were synthesized with 5% ratio of Cu and XRD patterns, SEM imagining

and nanoparticle size was analyzed. XRD patterns revealed peaks at around 44.5° which correspond to Fe diffraction, and 35° corresponds to the diffraction of Cu (Fig. 1) (Shubair et al., 2018; Tabrizian et al., 2019). The weak peaks at 35° and 65° can correspond to copper and iron oxide on the surface of the synthesized nanoparticle (Hussain et al., 2021; Shubair et al., 2018; Tabrizian et al., 2019). The intensities belonging to Fe and Copper can provide information on the presence and ratio of metals. According to SEM imagining shown in Fig. 2, the chain-like morphology of Fe^0 changed into an irregular shape and has worm shape structure on the core shape of Fe^0 .

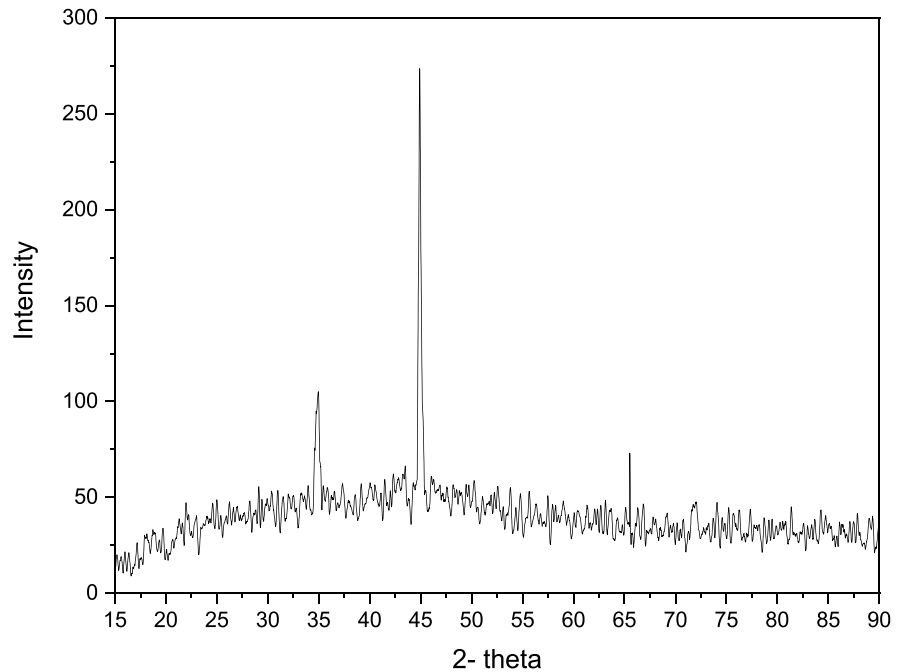
3.2 Life Cycle Assessment Results

The life cycle assessment was calculated for Fe/Cu nanoparticles synthesized by the borohydride method. The flowchart used in LCA is presented in Table 1, and the data were calculated for 1.0 kg Fe/Cu synthesis. The energy data were taken from Visentin et al. (2021). The comparative results of LCA calculations are presented in Table 2 and Fig. 3. The “mixture of reactant” sub-process in Fe/Cu synthesis presents the most significant negative environmental contribution in midpoint categories. The synthesis is based on the reaction of metal salts with borohydride solution. This high impact should be related to borohydride solution, as mentioned in a previous study by Visentin et al. (2021). The usage of borohydride reagent is the source of more than 87% of the synthesis’ environmental impact (Fig. 3). The washing” sub-process is followed with a holistic view. Stirring had the least contribution for each midpoint category. If washing and filtration are compared, filtration has a higher impact on ionizing radiation and freshwater eutrophication. The impact of filtration and washing was the same for human carcinogenic toxicity. Therefore, to remove borohydride reagent from the method, more greener synthesis should be used (Table 3).

3.3 Modeling of TCM Adsorption by Synthesized Fe/Cu Nanoparticle

The TCM removal efficiencies of the CCD study given in Table 4 were used to generate ANOVA analysis in Excel. Afterwards, the Design-Expert

Fig. 1 XRD pattern of synthesized Fe/Cu nanoparticles



13.0 program was used to analyze the compatibility of the experimental results with the predicted values and to interpret them graphically. Finally, the MATHCAD program was used to obtain optimum results. The ANOVA results are presented in Table 5. The adequacy and statistical significance of the developed CCD mode were examined according to the factors such as F -test, P value, coefficient of determination (R^2), adjusted R^2 , coefficient of variance (CV), and sufficient precision (AP). F -test is used to determine whether two variances (mean squared regression and mean squared residual) are equal. The adequacy of the model can be defined if the model has P values less than 0.05 (for this study 0.0004) and the lack of fit F (for this study 16) values higher than 0.05. The CV values less than 10 indicate a high precision and reliability of the experimental work performed. The CV of this study was determined as 3.79, which signifies the consistency of the model. In addition, the importance of the variables increases as the sum of squares value used to evaluate the acceptability of the model increases. The regression coefficient (R^2) of the study was 0.992, and the significance of the study was high, with a value of 3.6 E-09. The coefficients in Table 5 with lower P values than 0.05 were counted for determining whether the parameters were effective. Equation (6) was prepared according to Table 5,

where all independent variables (TCM concentration (x_1), Fe/Cu concentration (x_2) and reaction time (x_3)) were determined as effective:

$$y = 66.45 + 16.21x_1 + 3.85x_2 + 11.10x_3 + 5.00x_1x_2 - 2.50x_2x_3 - 1.93x_1^2 + 1.43x_1^2 - 2.06x_3^2 \quad (6)$$

The Pareto chart demonstrates the effect of independent variables on TCM removal. Equation (7) was used to prepare the Pareto charts (Fig. 4), where β_i is the coefficient of the independent variables (Ulucan-Altuntas et al., 2022):

$$P_i = \left(\frac{\beta_i^2}{\sum \beta_i^2} \right) \cdot 100 (i \neq 0) \quad (7)$$

Pareto charts were prepared based on independent parameters which are more than 1% effective. The Pareto chart can give the idea of which independent parameter affects the most, and for our study, it was revealed as TCM concentration and reaction time. This information can also be gathered from Table 5, and the highest coefficient belonged to TCM removal, followed by reaction time. In addition, the positive coefficient of these parameters indicates that they are effecting mainly linearly and positively.

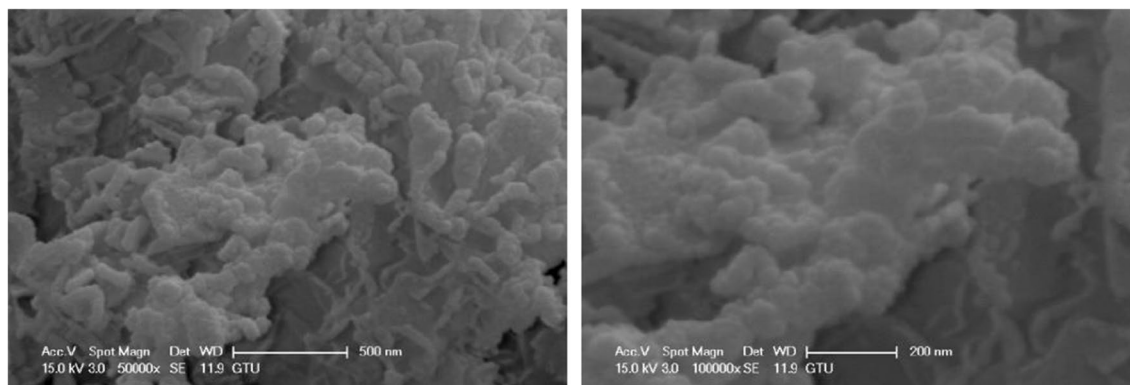


Fig. 2 SEM images of synthesized Fe/Cu nanoparticles

Three-dimensional (3D) response surface graphs illustrate the effect of two independent parameters factors on TCM removal at the midpoint ($\alpha=0$) of the other independent parameter not displayed on the graph. The surface graphs belonging to the combination of two independent parameters can be seen in Fig. 4. The TCM concentration lower than 175 $\mu\text{g/L}$ ($\alpha = -1$) could not be removed by

more than 50%, even if the Fe/Cu concentration was introduced at the highest studied concentration (650 mg/L) (Fig. 5a). Xu et al. (2017) studied TCM removal by Fe^0 and Fe/Al alloy particles, and it is reported that nZVI and Fe/Al can remove 178 $\mu\text{g/L}$ TCM concentration with 17% and 51% of removal efficiency, respectively. Synthesizing nZVI with a metal results in higher TCM removal.

Table 2 Flowchart used in LCA for Fe/Cu nanoparticle synthesis (* referenced from (Visentin & A.W. da S. Trentin, A.B. Braun, A. Thomé, 2021))

Used			Effluents		
Mixture of Reactants	FeCl	2.74 kg			
	BH4	3.19 kg			
	CuSO4	8.03 kg			
	Water	1.59 m3			
	Ethanol 95%	0.28 m3			
↓					
Stirring	Energy	0.0675 kWh*			
↓					
Filtration	Energy	0.0105 kWh*	→	Wastewater	1.87 m3
	Filter papers	2.00 kg			
↓					
Washing	Deionized water	0.11 m3	→	Wastewater	0.14 m3
	Ethanol 95%	0.03 m3			
↓					
Drying			→	Fe/Cu	1kg

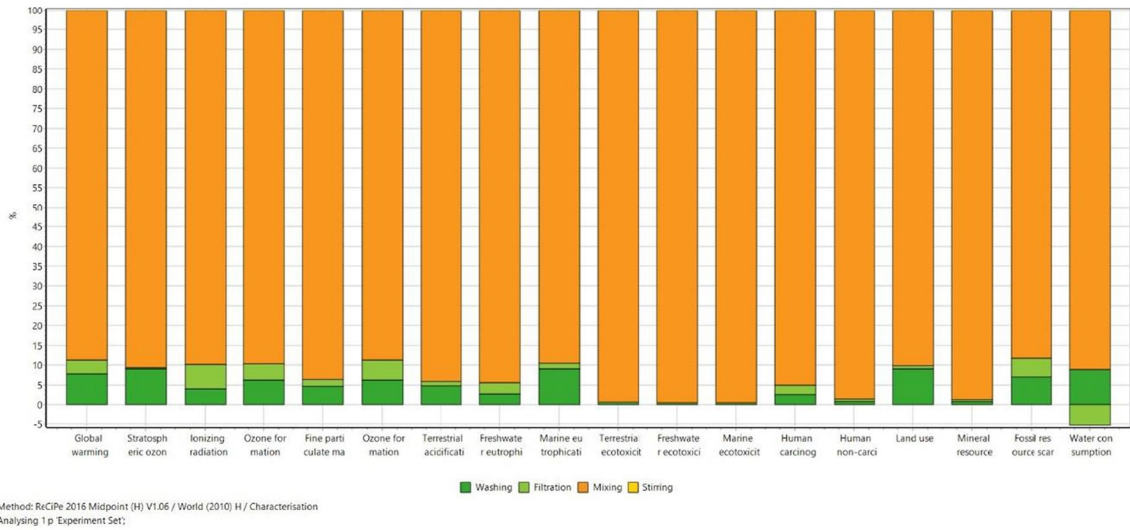


Fig. 3 Comparative results of midpoint categories

As predicted, for the higher TCM concentrations than 300 µg/L ($\alpha=0$), a higher concentration of Fe/Cu was required for higher removal efficiencies. As noted in the Pareto chart previously, TCM concentration and reaction time affected linearly; the lowest reaction time resulted in low removal

efficiencies (Fig. 5b). For the lowest TCM concentration (50 µg/L, $\alpha = -2$), the highest removal efficiency can be up to 40% by using 650 mg/L Fe/Cu nanoparticle and the highest reaction time (90 min, $\alpha = 2$). Wang et al. (2012) also stated that a reaction time greater than 48 h was required to remove total

Table 3 Results of midpoint categories

	Mixing	Stirring	Filtration	Washing	Unit
Global warming	238.1	0.04	9.4	20.8	kg CO ₂ eq
Stratospheric ozone depletion	0.0013	1.31E-08	5.15E-06	0.0001	kg CFC11 eq
Ionizing radiation	11.6	0.0003	0.8	0.5	kBq Co-60 eq
Ozone formation	0.8	9.78E-05	0.04	0.05	kg NO _x eq
Fine particulate matter formation	0.9	0.0003	0.02	0.04	kg PM _{2.5} eq
Terrestrial acidification	2.8	0.0002	0.03	0.1	kg NO _x eq
Freshwater eutrophication	0.2	4.43E-05	0.007	0.006	kg P eq
Marine eutrophication	0.2	2.77E-06	0.003	0.02	kg N eq
Terrestrial ecotoxicity	11,362.2	0.03	20.3	57.8	kg 1,4-DCB
Freshwater ecotoxicity	127.7	0.002	0.3	0.4	kg 1,4-DCB
Marine ecotoxicity	163.1	0.002	0.4	0.5	kg 1,4-DCB
Human carcinogenic toxicity	19.6	0.003	0.5	0.5	kg 1,4-DCB
Human non-carcinogenic toxicity	1970.1	0.05	9.8	18.2	kg 1,4-DCB
Land use	257.6	0.0004	2.2	26.1	m ² a crop eq
Mineral resource scarcity	6.1	1.86E-05	0.03	0.05	kg Cu eq
Fossil resource scarcity	47.1	0.01	2.5	3.8	kg oil eq
Water consumption	29.5	0.0003	-1.7	2.9	m ³

Table 4 CCD runs for TCM adsorption

Runs	Coded values			TCM removal efficiency	
	TCM Conc	Fe/Cu Conc	Reaction time	Actual values	Predicted values
	x_1	x_2	x_3	y	
1	-1	-1	-1	31.88	34.16
2	1	-1	-1	56.45	58.75
3	-1	1	-1	31.3	36.84
4	1	1	-1	62.9	81.44
5	-1	-1	1	63.88	63.51
6	1	-1	1	83.12	83.76
7	-1	1	1	55.33	56.21
8	1	1	1	95.57	96.47
9	-2	0	0	27.39	26.31
10	2	0	0	98.26	91.16
11	0	-2	0	65.33	64.50
12	0	2	0	92.23	79.89
13	0	0	-2	39.74	36.00
14	0	0	2	79.82	80.38
15	0	0	0	67.17	66.45
16	0	0	0	66.98	66.45
17	0	0	0	66.75	66.45
18	0	0	0	67.1	66.45
19	0	0	0	67.05	66.45
20	0	0	0	66.8	66.45

TCM by a composite of nZVI and activated carbon. Lu et al. (2006) reported that the adsorption equilibrium for TCM was reached at 150 min with carbon nanotubes. Figure 5c implies that reaction time is more effective in TCM removal than Fe/Cu concentration. In addition, the studies with low Fe/Cu nanoparticles require more reaction time to remove TCM (Fig. 5c). When the reaction time is high as

50 min, the effect of Fe/Cu concentration observed as less important; however, for the low reaction times, more Fe/Cu nanoparticle was required. In a study of Xu et al. (2017), the reaction mechanism by nZVI was proposed as not only adsorption but also degradation by losing Cl bond (8). The degradation by Fe/Cu bimetallic nanoparticles was considered as the same with Fe⁰:

Table 5 ANOVA results of CCD for TCM adsorption

	Coefficient	Standard error	P values	Importance
Intersection	66.45	0.972	1.1E-14	
x_1	16.21	0.610	1.3E-10	Very significant
x_2	3.85	0.610	8.75E-05	Very significant
x_3	11.10	0.610	5.37E-09	Very significant
$x_1 x_2$	5.00	0.862	1.7 E-4	Very significant
$x_1 x_3$	-1.09	0.862	0.236	-
$x_2 x_3$	-2.50	0.862	0.016	Significant
x_1^2	-1.93	0.486	0.003	Significant
x_2^2	1.43	0.486	0.014	Significant
x_3^2	-2.06	0.486	0.002	Significant

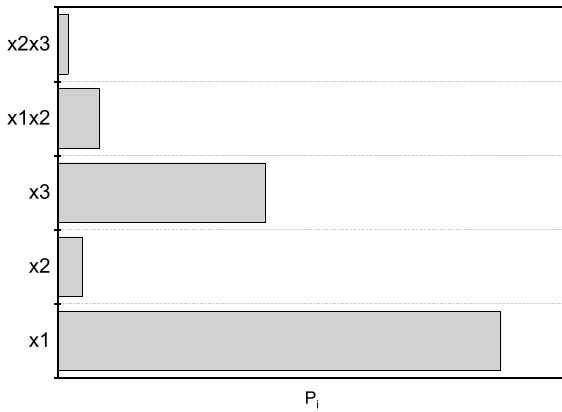
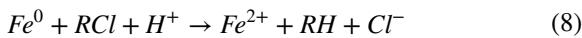


Fig. 4 Pareto chart for TCM removal by Fe/Cu nanoparticles



Dichloromethane was only observed in the studies with 50 min of reaction time ($\alpha=0$). Su et al. (2021) reported that dichloromethane was observed in removing carbon tetrachloride by Ni-doped nZVI with magnetic Fe₃O₄ after 35 min. The higher reaction time detected in this study can be explained as the experiments conducted at 30 min and 50 min of reaction time. However, it was not possible to observe for a study at a lower reaction time than 50 min. Another reason can be the low studied TCM concentration.

The model’s accuracy can be defined with the confidence interval (Ulucan-Altuntas & Debik, 2020), which can be calculated via Eq. (9):

$$CI = \bar{x} \pm z \frac{s}{\sqrt{n}} \tag{9}$$

where *CI* is the confidence interval, the mean expressed by \bar{x} , the confidence level value expressed by *z*, standard deviation expressed by *s*, and the number of samples defined as *n*. The value of *z* was selected as 1.96 (confidence level was 95%). CI was calculated as ± 3.0 . The optimum removal efficiency was obtained by 50 min of reaction time and 500 mg/L Fe/Cu concentration for 500 μ g/L. The reaction time which requires to achieve a concentration lower than 60 μ g/L can be 24 min by having $88.3 \pm 3.0\%$ removal efficiency. To better present the effect of Fe/Cu concentration for 500 μ g/L TCM concentration, the kinetic studies were conducted to calculate *k_t* values based on Eq. (10):

$$C = C_0 \cdot \exp(-k_t \cdot t) \tag{10}$$

where *C*₀ is the initial TCM concentration (μ g/L), *C* is the TCM concentrations at effluent (μ g/L) at *t* time (min), and *k_t* is the constant of pseudo-first-order (min^{-1}). The calculated kinetic values were given in Fig. 6. The regression coefficient (*R*²) of *k_t* of 100 mg/L, 200 mg/L, 400 mg/L, and 500 mg/L of Fe/Cu nanoparticles was 0.97, 0.95, 0.95, and 0.98, respectively. The highest *kt* value was 0.133 min^{-1} , belonging to 500 mg/L of Fe/Cu concentration. Total removal can be obtained for 50 min, 70 min for 400, and 500 mg/L, while more than 90 min was required for higher removal rates for Fe/Cu concentration lower than 200 mg/L (Fig. 5). This increase in the removal efficiencies can be attributed to the increment of active sites when the Fe/Cu concentration is higher (Su et al., 2021).

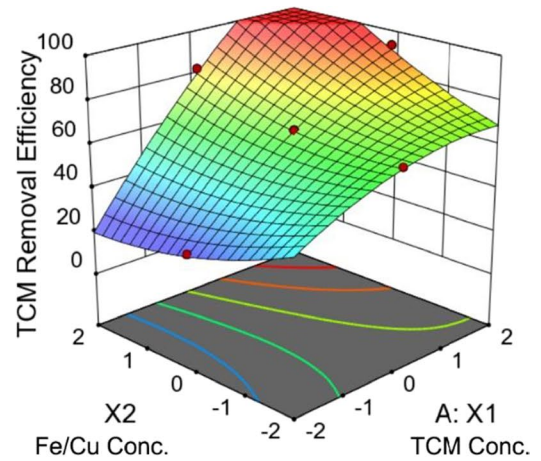
4 Conclusion

In the present study, Fe/Cu bimetallic nanoparticles have been successfully prepared based on the modified nZVI synthesis method and were used to remove TCM from aqueous solution. RSM with CDD proved to be a powerful tool for optimizing the operational conditions of TCM removal efficiency using Fe/Cu. The model was statistically significant at 95% confidence level. RSM revealed that the most effective factor on the removal of TCM was TCM concentration > reaction time. The optimum adsorption conditions were TCM concentration (500 μ g/L), Fe/Cu concentration (500 mg/L), and reaction time (50 min). The reaction time can be lowered through synthesizing bimetallic nanoparticles as supported on a low-cost adsorbent (i.e., activated carbon), and this will let the process be available for column tests. LCA was applied to determine the impacts on mid-point environmental categories. The highest impact occurred through the stage of “mixture of reagents.” The reason is regarded as the usage of borohydride reagent. More greener synthesis method without using borohydride should be used.

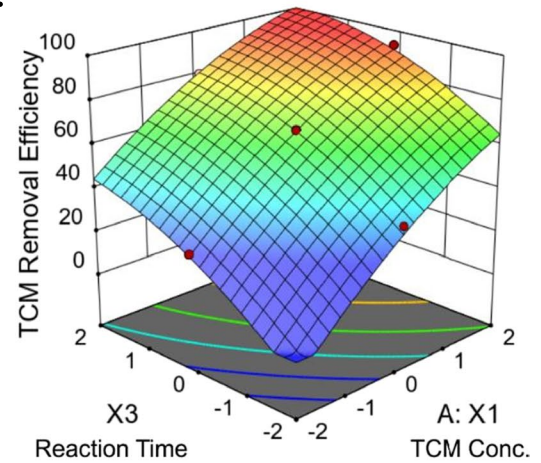
Funding Open access funding provided by Università degli Studi di Padova within the CRUI-CARE Agreement. The authors thank Bandirma Onyedi Eylul University for supporting to buy the licensed version of SimaPro 9.3.0.2 software.

Fig. 5 Effects of Fe/Cu concentration and TCM concentration on TCM Removal efficiency (Reaction time is 50 min). **(b)** Effects of reaction time and TCM concentration on TCM Removal efficiency (Fe/Cu concentration is 350 mg/L). **(c)** Effect of reaction time and Fe/Cu concentration on TCM removal efficiency (TCM Concentration is 300 $\mu\text{g/L}$)

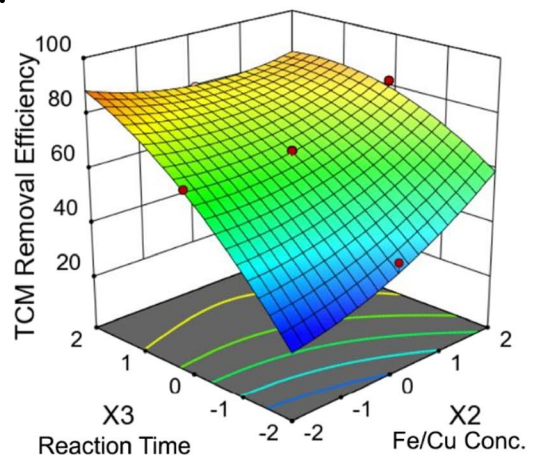
a.



b.



c.



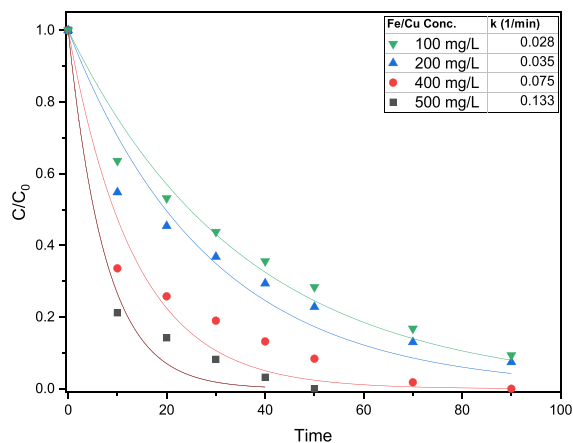


Fig. 6 The removal efficiencies for different Fe/Cu concentrations versus reaction time for 500 µg/L TCM concentration

Kubra Ulucan-Altuntas was supported by Marie S. Curie Fellowship during the submission of this study.

Data Availability The authors confirm that the data supporting the findings of this study are available within the article.

Declarations

Competing Interests The authors declare no competing interests.

Open Access This article is licensed under a Creative Commons Attribution 4.0 International License, which permits use, sharing, adaptation, distribution and reproduction in any medium or format, as long as you give appropriate credit to the original author(s) and the source, provide a link to the Creative Commons licence, and indicate if changes were made. The images or other third party material in this article are included in the article's Creative Commons licence, unless indicated otherwise in a credit line to the material. If material is not included in the article's Creative Commons licence and your intended use is not permitted by statutory regulation or exceeds the permitted use, you will need to obtain permission directly from the copyright holder. To view a copy of this licence, visit <http://creativecommons.org/licenses/by/4.0/>.

References

- Benítez, J. S., Rodríguez, C. M., & Casas, A. F. (2021). Disinfection byproducts (DBPs) in drinking water supply systems: A systematic review. *Physics and Chemistry of the Earth*, 123. <https://doi.org/10.1016/j.pce.2021.102987>.
- Bilgili, L., Kuzu, S. L., Çetinkaya, A. Y., & Kumar, P. (2019). Evaluation of railway versus highway emissions using LCA approach between the two cities of Middle Anatolia. *Sustainable Cities and Society*, 49, 101635. <https://doi.org/10.1016/j.scs.2019.101635>
- Çetinkaya, A. Y. (2020). Life cycle assessment of environmental effects and nitrate removal for membrane capacitive deionization technology. *Environmental Monitoring and Assessment*, 192, 543. <https://doi.org/10.1007/s10661-020-08501-0>
- Çetinkaya, A. Y., Bilgili, L., & LeventKuzu, S. (2018). Life cycle assessment and greenhouse gas emission evaluation from Aksaray solid waste disposal facility. *Air Quality Atmosphere and Health*, 11, 549–558. <https://doi.org/10.1007/s11869-018-0559-3>
- Cetinkaya, A. Y., Kuzu, S. L., & Bilgili, L. (2022). Development of an MFC-biosensor for determination of Pb+2: An assessment from computational fluid dynamics and life cycle assessment perspectives. *Environmental Monitoring and Assessment*, 194, 245. <https://doi.org/10.1007/s10661-022-09894-w>
- da Cunha, G. C., Romão, L. P. C., Santos, M. C., Araújo, B. R., Navickiene, S., & de Pádua, V. L. (2010). Adsorption of trihalomethanes by humin: Batch and fixed bed column studies. *Bioresour Technol*, 101, 3345–3354. <https://doi.org/10.1016/j.biortech.2009.11.096>
- DomínguezHenao, L., Turolla, A., & Antonelli, M. (2018). Disinfection by-products formation and ecotoxicological effects of effluents treated with peracetic acid: A review. *Chemosphere*, 213, 25–40. <https://doi.org/10.1016/j.chemosphere.2018.09.005>
- Dong, H., Xie, Y., Zeng, G., Tang, L., Liang, J., He, Q., Zhao, F., Zeng, Y., & Wu, Y. (2016). The dual effects of carboxymethyl cellulose on the colloidal stability and toxicity of nanoscale zero-valent iron. *Chemosphere*, 144, 1682–1689. <https://doi.org/10.1016/j.chemosphere.2015.10.066>
- Dong, Q., Dong, H., Li, Y., Xiao, J., Xiang, S., Hou, X., & Chu, D. (2022). Degradation of sulfamethazine in water by sulfite activated with zero-valent Fe-Cu bimetallic nanoparticles. *Journal of Hazardous Materials* 128601. <https://doi.org/10.1016/j.jhazmat.2022.128601>
- Finkbeiner, M., Inaba, A., Tan, R., Christiansen, K., & Klüppel, H.-J. (2006). The New International Standards for Life Cycle Assessment: ISO 14040 and ISO 14044. *International Journal of Life Cycle Assessment*, 11, 80–85. <https://doi.org/10.1065/lca2006.02.002>
- Hauschild, M. Z., Rosenbaum, R. K., & Olsen, S. I. (2017). Life cycle assessment: Theory and practice, life cycle assess. Theory and Practice 1–1216. <https://doi.org/10.1007/978-3-319-56475-3>.
- Hussain, S., Aneggi, E., Goi, D., & Trovarelli, A. (2021). Bimetallic Cu/Fe catalysts for ibuprofen mineralization. *Catalysts*, 11, 1383. <https://doi.org/10.3390/CATAL11111383/S1>
- Kahraman, B. F., Altin, A., & Ozdogan, N. (2022). Remediation of Pb-diesel fuel co-contaminated soil using nano/bio process: Subsequent use of nanoscale zero-valent iron and bioremediation approaches. *Environmental Science and Pollution Research*, 2022(1), 1–15. <https://doi.org/10.1007/S11356-022-18857-0>
- Lu, C., Chung, Y. L., & Chang, K. F. (2006). Adsorption thermodynamic and kinetic studies of trihalomethanes on multiwalled carbon nanotubes. *Journal of Hazardous Materials*, 138, 304–310. <https://doi.org/10.1016/j.jhazmat.2006.05.076>

- Matsui, Y., Nakao, S., Sakamoto, A., Taniguchi, T., Pan, L., Matsushita, T., & Shirasaki, N. (2015). Adsorption capacities of activated carbons for geosmin and 2-methylisoborneol vary with activated carbon particle size: Effects of adsorbent and adsorbate characteristics. *Water Research*, 85, 95–102. <https://doi.org/10.1016/J.WATRES.2015.08.017>
- Shubair, T., Eljamal, O., Khalil, A. M. E., Tahara, A., & Matsunaga, N. (2018). Novel application of nanoscale zero valent iron and bimetallic nano-Fe/Cu particles for the treatment of cesium contaminated water. *Journal of Environmental Chemical Engineering*, 6, 4253–4264. <https://doi.org/10.1016/j.jece.2018.06.015>
- Sriboonnak, S., Induvas, P., Wattanachira, S., Rakruam, P., Siyasukh, A., Pumas, C., Wongrueng, A., & Khan, E. (2021). Trihalomethanes in water supply system and water distribution networks, *International Journal of Environmental Research and Public Health* 18. <https://doi.org/10.3390/IJERPH18179066>.
- Su, J., Chen, H., Wang, J., & Yang, Q. (2021). Enhanced dechlorination of carbon tetrachloride by Ni-doped zero-valent iron nanoparticles @ magnetic Fe₃O₄ (Ni₄/Fe@Fe₃O₄) nanocomposites. *Colloids and Surfaces A: Physicochemical and Engineering Aspects*, 623, 126691. <https://doi.org/10.1016/J.COLSURFA.2021.126691>
- Tabrizian, P., Ma, W., Bakr, A., & Rahaman, M. S. (2019). pH-sensitive and magnetically separable Fe/Cu bimetallic nanoparticles supported by graphene oxide (GO) for high-efficiency removal of tetracyclines. *Journal of Colloid and Interface Science*, 534, 549–562. <https://doi.org/10.1016/j.jcis.2018.09.034>
- Tural, B., Ertas, E., Güzel, M., & Tural, S. (2021). Effect of structural differences of pumice on synthesis of pumice-supported nFe₀: Removal of Cr (VI) from water. *Applied Water Science*, 11, 1–11. <https://doi.org/10.1007/S13201-021-01458-6/TABLES/4>
- Ulucan-Altuntas, K. (2019). Removal of humic substances by nano zero-valent iron supported on activated carbon and implementation of response surface methodology. *Desalination and Water Treatment* 166 <https://doi.org/10.5004/dwt.2019.24508>.
- Ulucan-Altuntas, K., YaziciGuvenc, S., Can-Güven, E., Ilhan, F., & Varank, G. (2022). Degradation of oxytetracycline in aqueous solution by heat-activated peroxydisulfate and peroxymonosulfate oxidation. *Environmental Science and Pollution Research*, 29, 9110–9123. <https://doi.org/10.1007/S11356-021-16157-7>
- Ulucan-Altuntas, K., & Debik, E. (2018). Borohydride method modification in synthesizing nano zero valent iron and its application in DDT removal. *Environmental Science and Pollution Research* 25. <https://doi.org/10.1007/s11356-018-2989-8>.
- Ulucan-Altuntas, K., & Debik, E. (2020). Dechlorination of dichlorodiphenyltrichloroethane (DDT) by Fe/Pd bimetallic nanoparticles: Comparison with nZVI, degradation mechanism, and pathways. *Frontiers of Environmental Science and Engineering* 14. <https://doi.org/10.1007/s11783-019-1196-2>.
- Ulucan-Altuntas, K., & Kuzu, S. L. (2019). Modelling and optimization of dye removal by Fe/Cu bimetallic nanoparticles coated with different Cu ratios. *Materials Research Express* 6. <https://doi.org/10.1088/2053-1591/ab4bb5>.
- Ulucan-Altuntas, K., Debik, E., Ustundag, C. B., Guven, M. D., & Gocen, K. A. (2020). Effect of visible light on the removal of trichloromethane by graphene oxide. *Diamond and Related Materials* 107814. <https://doi.org/10.1016/j.diamond.2020.107814>.
- Venkateshaiah, A., Silvestri, D., Waclawek, S., Ramakrishnan, R. K., Krawczyk, K., Saravanan, P., Pawlyta, M., Vinod, V. V., Černík, M., & Dionysiou, D. D. (2021). A comparative study of the degradation efficiency of chlorinated organic compounds by bimetallic zero-valent iron nanoparticles. *Environmental Science: Water Research and Technology*, 8, 162–172. <https://doi.org/10.1039/D1EW00791B>
- Visentin, C., da Trentin, A. W. S., Braun, A. B., & Thomé, A. (2021). Life cycle sustainability assessment of the nanoscale zero-valent iron synthesis process for application in contaminated site remediation. *Environmental Pollution*, 268, 115915. <https://doi.org/10.1016/J.ENVPOL.2020.115915>
- Wang, Y., Huang, Q., Xian, Q., & Sun, C. (2012). Preparation of activated carbon fiber supported nanoscale Fe₀ for simultaneous adsorption and dechlorination of chloroform in water. *Advances in Materials Research*, 399–401, 1386–1391. <https://doi.org/10.4028/WWW.SCIENTIFIC.NET/AMR.399-401.1386>
- Xia, Q., Zhang, D., Yao, Z., & Jiang, Z. (2022). Revealing the enhancing mechanisms of Fe–Cu bimetallic catalysts for the Fenton-like degradation of phenol. *Chemosphere*, 289, 133195. <https://doi.org/10.1016/J.CHEMOSPHERE.2021.133195>
- Xu, J., Pu, Y., Yang, X. J., Wan, P., Wang, R., Song, P., & Fisher, A. (2017). Rapid removal of chloroform, carbon tetrachloride and trichloroethylene in water by aluminum–iron alloy particles*. 39:2882–2890. <https://doi.org/10.1080/09593330.2017.1369577>.
- Zhang, L., Xu, L., Zeng, Q., Zhang, S. H., Xie, H., Liu, A. L., & Lu, W. Q. (2012). Comparison of DNA damage in human-derived hepatoma line (HepG2) exposed to the fifteen drinking water disinfection byproducts using the single cell gel electrophoresis assay. *Mutation Research Genetic Toxicology and Environmental Mutagenesis*, 741, 89–94. <https://doi.org/10.1016/J.MRGENTOX.2011.11.004>

Publisher's Note Springer Nature remains neutral with regard to jurisdictional claims in published maps and institutional affiliations.